New rare earth silicate crystals: $Dy_2MoSi_2Al_4O_{16}$, compounds in the systems R_2O_3–SiO_2–PbO, and a new form of R_2SiO_5

B. M. WANKLYN, F. R. WONDRE
Clarendon Laboratory, Oxford, UK

G. B. ANSELL
Michelson Laboratory, China Lake, California, USA

W. DAVISON
School of Physics, The University, Newcastle-upon-Tyne, UK

The growth of crystals of a new cubic compound, $Dy_2MoSi_2Al_4O_{16}$, and of R_2SiO_5 (R = Dy, Tb, Gd) with a new structure is reported. Flux growth studies in the systems R_2O_3–SiO_2–PbO are also described. These have yielded single crystals of two new families of compounds: $PbR_4Si_5O_{17}$, with a monoclinic structure, and apatite-related phases of composition between $Pb_{1.4}Er_{2.93}Si_{3.6}O_{13}$ and $Pb_{1.8}Er_{2.5}Si_{3.7}O_{13}$ for R = Er. The compounds are characterized by X-ray powder patterns, single crystal X-ray data, and EPMA.

1. Introduction

Rare earth silicate compounds have been extensively investigated [1-9] and their structures have been the subject of a recent review [10]. They are potentially valuable on account of their low temperature magnetic properties and as laser host materials.

$Dy_2MoSi_2Al_4O_{16}$ and the new form of R_2SiO_5 (R = Dy, Tb, Gd) were obtained in the course of flux growth studies of rare earth silicates from the fluxes PbO, MoO_3 and PbF_2, or mixtures of these.

The phase diagrams for R_2O_3–SiO_2 (R = Er, Dy and Gd) and PbO–SiO_2 have been reported [11]. In the present work, crystal growth in the three-component systems R_2O_3–SiO_2–PbO has been investigated, and the starting compositions and growth conditions for the new compounds are reported.

2. Chemicals

The chemicals used were: Rare Earth Products 99.9% pure rare earth oxides, BDH "Analar" grade MoO_3, Al_2O_3, PbO, PbO_2, precipitated SiO_2 (containing 12% H_2O), Koch-Light SiO_2 (granular) and Johnson Matthey Grade 2 PbF_2.

3. Equipment

The furnaces, control equipment [12], and the use of sillimanite muffles [13] have been reported previously. The crucibles were of pure platinum, 0.5 mm in wall thickness, each provided with a closely fitting lid.

4. Experiments and results

To provide oxidizing conditions during heating, a few wt % PbO was included as PbO_2. The crucibles were placed in a sillimanite muffle in the furnace and were heated to the soak temperature at about 100 K h^{-1}. At the end of the cooling programme, the furnace was cooled to room temperature at 100 K h^{-1}.

4.1. $Dy_2MoSi_2Al_4O_{16}$

The crystals grew on the outer surface of a platinum lid which covered a crucible containing Dy_2O_3, SiO_2, MoO_3 and PbO. The melt composition and furnace programme is given in (a) of Table I.

A further batch of the crystals was obtained when a different melt composition was used (b, Table I) but attempts to grow the compound by evaporation of the flux from a melt containing PbF_2 and its components yielded only garnets.

TABLE I Starting compositions, furnace programmes and crystal products

Composition of mixture	Crucible volume (cm^3)	t_{max} (°C)	Soak period (h)	Rate of cooling ($K\ h^{-1}$)	Duration (h)	Final temperature (°C)	Crystal products
(a) 3.3 g Dy_2O_3, 1.9 g SiO_2 (BDH precipitated), 33.5 g MoO_3, 33.5 g PbO, 2.2 g PbO_2, (Al supplied by vapour transport)	40	1280	6	2 then 5	16 50	1000	$Dy_2MoSi_2Al_4O_{16}$. Isotropic colourless crystals, 1 to 2 mm, grew on crucible lid
(b) 2.4 g Dy_2O_3, 0.7 g SiO_2 (BDH precipitated), 8 g MoO_3, 2.8 g PbO, 0.7 g PbO_2, 11.2 g PbF_2 (Al supplied by vapour transport)	20	1250	12	1.4 then 5	30 30	1060	$Dy_2MoSi_2Al_4O_{16}$ crystals, identical to those described above, grew on the lid
(c) 0.55 g Er_2O_3, 1.7 g SiO_2 (BDH precipitated), 5.05 g PbO, 0.2 g PbO_2	10	1235	6	1.8	270	750	$PbEr_4Si_5O_{17}$. Transparent pink platey rods in clear glass at surface and base, up to (6 × 3 × 0.5) mm^3
(d) 3.55 g Y_2O_3, 12 g SiO_2 (BDH precipitated, dehydrated), 37.2 g PbO, 4.8 g PbO_2	100	1295	14	1 then 1.5	170 170	870	$PbY_4Si_5O_{17}$. Platey rods grew at the surface
(e) 1.8 g Dy_2O_3, 2.1 g MoO_3, 18 g PbF_2, 5 g PbO, 0.5 g PbO_2 (Si supplied by vapour transport into melt)	10	1270	70	—	—	—	New form of Dy_2SiO_5. Pale yellow rods, twinned, shown in Fig. 1a
(f) 1.2 g Dy_2O_3, 0.4 g SiO_2 (BDH precipitated), 16.5 g PbF_2, 0.5 g PbO_2	10	1290	100	—	—	—	New form of Dy_2SiO_5. Pale yellow rods, twinned
(g) 2 g Gd_2O_3, 0.4 g SiO_2 (BDH precipitated), 26 g PbF_2, 6 g PbO, 1.4 g PbO_2	10	1250	1	1	200	1050	New form of Gd_2SiO_5. Rather formless colourless crystals, twinned, 2 mm on edge
(h) 6.8 g Tb_4O_7, 1.8 g SiO_2 (BDH precipitated), 16.8 g MoO_3, 38 g PbF_2, 4 g PbO, 1 g PbO_2	50	1250	24	1.4 then 5	30 30	1060	New form of Tb_2SiO_5. Brown transparent faceted rods shown in Fig. 1b

The crystals were colourless, optically isotropic, and 1 to 2 mm on edge, with no distinct facets. The formula $Dy_2MoSi_2Al_4O_{16}$ was derived from EPMA (Table II). The occurrence of the crystals was accounted for on the basis that the oxides of Dy, Mo and Si had been transported to the growth sites by creeping of the melt, while Al had been provided by a vapour species which resulted from the reaction of PbO or PbF_2 with Al_2O_3 powder around the crucible [14]. Attempts were made to obtain the compound by sintering the component oxides. Material was heated in a sealed platinum tube to avoid loss of MoO_3, which sublimes at 600°C, but the tube burst on heating. 10 wt % additional MoO_3 to that required by the formula was then included in a sample to compensate for loss on heating, and the powder, in a platinum crucible with tightly fitting lid, was heated at 300 k h^{-1} to 1300°C, and held for 12 h. The powder pattern of the sinter very closely resembled that of the crystals, as shown in Table III.

X-ray powder pattern data were obtained with a Debye-Scherrer camera using Cu$K\alpha$ radiation. The film was calibrated by mixing powdered silicon with the sample. The pattern was

TABLE II EPMA data for the crystals

Formula	Formula requires (%)		EPMA found (%)
$Dy_2MoSi_2Al_4O_{16}$	Dy_2O_3	44.3	43.7
	MoO_3	17.1	17.7
	SiO_2	14.3	14.8
	Al_2O_3	24.3	23.2
$PbEr_4Si_5O_{17}$	Er	51.9	51.1
	Si	10.9	9.2
	Pb	16.1	16.6
Phase B: Er-rich			
$Pb_{1.4}Er_{2.93}Si_{3.6}O_{13}$	Er	45	45
	Si	9.3	9.4
	Pb	26.6	28
Phase B: Pb-rich			
$Pb_{1.8}Er_{2.5}Si_{3.7}O_{13}$	Er	37.9	37.4
	Si	9.4	9.2
	Pb	33.8	
Dy_2SiO_5	Dy	75	75.7
			Pb 0.1
Gd_2SiO_5	Gd	74.4	74.7
	Si	6.6	5.9
			Pb 0.4

indexed on the basis of a primitive cubic unit cell, $a_0 = 9.254$ Å, which gave excellent agreement between observed and calculated values of $\sin^2\theta$ (Table III). Systematic absences found on $h0l$, $h1l$ and $h2l$ Weissenberg photographs show that the general conditions for limiting possible reflections are $h00\bigcirc$, $h = 2n$; $hk0\bigcirc$, $h + k = 2n$. This gives $Pn3$ and $Pn3m$ as possible space-groups, in either of which the atoms occupy a mixture of general and special positions.

4.2. R_2SiO_5 (R = Dy, Tb, Gd) with a new crystal structure

In the course of an investigation into the flux growth of rare earth silicates by evaporation of the flux from mixtures of PbF_2 and the component oxides, a group of rare earth silicates giving closely related powder patterns, distinct from those already known [4, 10] and with R = Dy, Tb and Gd, was obtained.

The crystals which grew as a result of evaporation of PbF_2 from melts containing PbF_2, R_2O_3 (R = Dy, Tb, Gd) with SiO_2 present in varied proportions, were usually either R_2SiO_5 (R =

TABLE III X-ray powder pattern data for crystalline $Dy_2MoSi_2Al_4O_{16}$ and for the sintered material of this composition. Also single crystal X-ray data

Sintered material		Crystal material				
Intensity (estimated)	d_{obs}	Intensity (estimated)	d_{obs}	$\sin^2\theta_{obs}$	$\sin^2\theta_{calc}$	hkl
VS	5.35	VS	5.35	0.021	0.021	111
VW	4.64	VW	4.64	0.028	0.028	002
VS	3.78	VS	3.78	0.042	0.042	112
S	3.27	S	3.27	0.055	0.056	022
MS	3.02	VW	3.02			N.I.
S	2.79	S	2.79	0.076	0.076	113
M	2.67	M	2.67	0.083	0.083	222
VW	2.55		—			N.I.
W	2.47	W	2.47	0.097	0.097	123
M	2.313	M	2.316	0.111	0.111	004
W	2.178	W	2.183	0.124	0.125	114, 033
S	2.119	S	2.127	0.131	0.132	133
W	2.067	W	2.072	0.138	0.139	024
W	1.970	W	1.978	0.152	0.153	233
S	1.886	S	1.894	0.166	0.167	224
S	1.779	S	1.781	0.187	0.187	115, 333
MS	1.687	MS	1.692	0.208	0.208	125
W	1.600		—			N.I.
S	1.633	S	1.637	0.222	0.222	044
MS	1.563	MS	1.565	0.243	0.243	135
W	1.500	W	1.502	0.264	0.264	116, 235
W	1.461	W	1.463	0.277	0.278	026

$a_0 = 9.254$ Å.
Space group: $Pn3$ or $Pn3m$.

Dy, Tb) with the Er_2SiO_5 structure [4], or the apatite compounds of formula approximately $PbR_4(SiO_4)_3O$ [9]. The compounds R_2SiO_5 with the new structure were obtained from only four batches of over 40 of this kind, and it appears that their structures must be somewhat unstable by comparison with those of the other silicate phases under these growth conditions. No special feature was associated with batches which produced them. Batch compositions and growth procedures are given in Table I (e, f, g and h). In one case, Si was provided by a vapour species [13]. The flattened rods with faceted ends, up to 20 mm × 2.5 mm × 0.3 mm (Fig. 1), were transparent, and

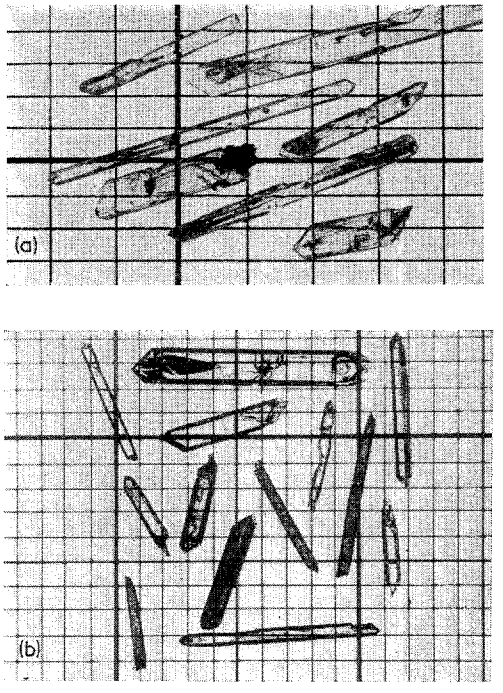

Figure 1 Crystals of R_2SiO_5 with the new structure (a) Dy_2SiO_5, (2 mm × 1 mm grid). (b) Tb_2SiO_5 (1 mm × 1 mm grid).

examination between crossed polarizers showed that they were intimately twinned; the twin structure was not related to the crystal facets and thus was apparently due to a crystallographic transition below the growth temperature. Some crystals were heated at 1700°C for a short period. The crystals did not alter in appearance and the X-ray powder pattern was unchanged. EPMA indicated that Pb was present only as a trace impurity and not as part of the formula Table II).

Initial EPMA results for the compound with Dy indicated a low silicon content, and this was previously reported to have the formula Dy_4SiO_8 [13]. Subsequently, EPMA was carried out using as a standard a crystal of Dy_2SiO_5, which was identified by comparison of its powder pattern with published data [4, 8]. The EPMA counts on the standard and on the unknown crystal for both Dy and Si were found to be in close agreement:

	Dy_2SiO_5	unknown Dy phase
Dy	50020	50291
Si	4166	4111

It was thus established that the unknown phase was a new form of Dy_2SiO_5. In addition EPMA data for the Gd compound was in good agreement with the formula Gd_2SiO_5 (Table II). In view of the close relationship of the powder patterns of the three compounds with R = Dy, Gd and Tb, given in Table IV, it was deduced that the terbium compound also has the formula Tb_2SiO_5.

TABLE IV X-ray powder pattern data for R_2SiO_5 with the new structure (R = Dy, Tb, Gd)

Intensity (estimated)	Gd_2SiO_5 d_{obs}	Tb_2SiO_5 d_{obs}	Dy_2SiO_5 d_{obs}
VW	5.49	5.44	5.38
VW	4.78	4.74	4.71
S	4.34	4.34	4.31
VW	3.83	3.82	3.79
VW	3.70	3.70	3.66
VW	—	3.60	3.59
VW	3.358	3.349	3.324
VW	—	3.246	3.229
W	3.071	3.059	3.043
W	—	—	3.015
VS	2.903	2.897	2.881
MS	2.781, 2.752	2.773	2.753
MS	2.711, 2.678	2.689	2.665
VW	—	2.409	2.383
W	2.205	2.194	2.160
W	2.124	2.108	2.093
S	1.980	—	1.964
W	1.894	1.885	1.871
W	1.848	1.833	1.824
M	1.765	1.758	1.751

The recent review by Felsche [10] describes two series of isostructural compounds of formula

R_2SiO_5, one with the smaller rare earth ions Lu^{3+} to Tb^{3+}, and the second, with the larger rare earth ions Tb to La, having a different structure. The R_2SiO_5 compounds reported in this paper form a third series with rare earth ions overlapping the end members of each of the two previous series.

4.3. Compounds in the system R_2O_3–SiO_2–PbO (R = Er)

Starting compositions in the system Er_2O_3–SiO_2–PbO are indicated in Fig. 2. As observed previously [15], the solubility of rare-earth complex oxides in PbO-based fluxes at 1260 to 1300°C is typically 3 to 5 wt % R_2O_3. In this work, slightly higher solubilities were noted, the maximum being 7 wt %.

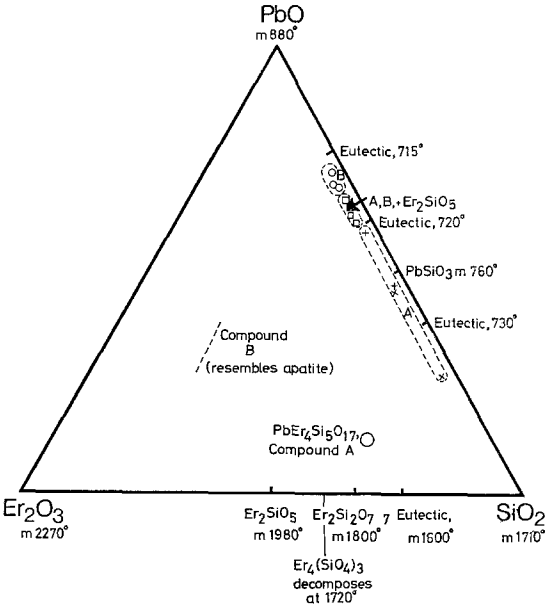

Figure 2 Composition diagram Er_2O_3–SiO_2–PbO. ×: compositions resulting in $PbEr_4Si_5O_{17}$, phase A. ○: compositions resulting in the apatite-like phase B. □: compositions resulting in Phase A, Phase B and sometimes Er_2SiO_5.

At the end of the crystal growth experiments, the flux and crystals were removed mechanically. With starting compositions in region A in Fig. 2, transparent rods 5 to 12 mm in length grew across the melt surface. These were typically 1 to 3 mm in width and 1 to 2 mm in depth. The flux broke away fairly readily from the crystals which were cleaned by soaking in warm 1:10 HNO_3 solution for 20 h. Usually some facets were evident at the upper surface. Occasionally growth occurred at the crucible base or as sheets growing into the melt. The crystals were brittle and cracked easily. They showed uniform extinction along their axes and the colour was characteristic of the rare earth ion. A starting composition and furnace programme which yielded good crystals of phase A are given in Table I(c). It was found that crystals did not grow satisfactorily when Koch-Light granular SiO_2 powder was used. Possibly, nuclei remained in the melt, providing too many growth centres. Melts containing precipitated SiO_2 or finely ground silica gel invariably produced Phase A with starting compositions in region A.

EPMA showed that Pb was an integral part of the formula, $PbEr_4Si_5O_{17}$ (Table II). A stoichiometric mixture of the components was sintered at 1250°C for 20 h, and the powder pattern of the material that resulted very closely resembled that of the crystals (Table V), both as to intensity and spacing.

Single crystal oscillation and Weissenberg photographs have shown that this material is monoclinic. Cell dimensions were measured on a General Electric Single Crystal Orienter and found to be $a = 5.534$, $b = 19.58$, $c = 6.960$ Å, $\beta = 107.2°$. There are systematic absences for $0k0$ reflections ($k = 2n + 1$). Single-crystal data were collected and a structure determination has shown the space-group to be $P2_1/m$ with two $PbEr_4Si_5O_{17}$ units per unit cell. These data have been refined by full-matrix least-squares structure-factor calculations to an R value of 0.090. The two erbium atoms have co-ordinates (0.201, 0.039, 0.383) and (0.848, 0.156, 0.014). Lead occupies the m symmetry position of 0.204, 0.250, 0.708. In the unit cell there are $(Si_3O_{10})^{8-}$ anions with mirror symmetry and $(Si_2O_7)^{6-}$ anions which are centrosymmetric; the formula may be written $PbEr_4(Si_2O_7)\ (Si_3O_{10})$. The refinement is being continued and will be reported elsewhere.

The crystals obtained in region B were hexagonal rods, up to 1 mm in thickness and up to 1 cm long. They were transparent and showed uniform extinction along their axes. They usually grew at the melt surface. Their surfaces were extensively etched after 2 h in warm 1:10 HNO_3 solution. The X-ray powder patterns have been indexed on the basis of an apatite-like unit cell (Table VI) and powder pattern data for gadolinium oxyapatite is included to show the similarity.

The X-ray powder pattern lines were broad,

TABLE V X-ray powder pattern data for $PbEr_4Si_5O_{17}$ crystals, for sintered material of this composition, and for crystals of this phase with R = Dy and Y

hkl	I/I_0	$PbY_4Si_5O_{17}$ d_{obs}	$PbEr_4Si_5O_{17}$ d_{obs}	$PbDy_4Si_5O_{17}$ d_{obs}
021	20	5.44	5.45	5.42
100	18	5.29	5.27	5.27
031	25	4.61	4.63	4.59
$12\bar{1}$	13	4.35	4.35	4.38
041, $13\bar{1}$	21	3.90	3.91	3.93
111	16	3.56	3.56	3.60
121	31	3.390	3.395	3.422
$11\bar{2}$	34	3.191	3.200	3.199
150	100	3.129	3.137	3 151
$12\bar{2}$	17	3.070	3.076	3.093
061, 032, 141, $13\bar{2}$	27	2.921	2.918	2.942
$21\bar{1}$, $16\bar{1}$, 042	52	2.713	2.716	2.741
$22\bar{1}$, 200	25	2.643	2.639	2.667
071	9	2.569	2.571	2.573
102	12	2.459	2.461	2.477
$17\bar{1}$	13	2.425	2.426	2.424
062	16	2.310	2.313	2.322
$10\bar{3}$	20	2.265	2.270	2.286
250, $18\bar{1}$	60	2.190	2.192	2.202
072	26	2.122	2.125	2.132
162, 0, 10, 0	43	1.955	1.966	1.963

TABLE VI X-ray powder pattern data for Phase B with R = Er and for Gd oxyapatite

Phase B with R = Er			Oxyapatite $Pb_{0.2}Gd_{4.8}Si_{2.6}Al_{0.2}O_{13}$ [9]		
d_{obs}	Intensity (estimated)	*hkl*	d_{obs}	Intensity (estimated)	*hkl*
4.15	W	200	4.09	MS	200
3.90	M	111	3.90	W	111
3.37	W	002	3.44	W	002
3.13	S	012	3.176	S	012
			3.088	S	120
2.85	VS	121	2.825	VS	121
2.76	S	112	2.786	S	112
			2.727	S	030
2.30	VW	122			
			2.646	VW	022
2.14	VW	302			
			2.146	VW	131
			2.069	VW	113
2.08	VW	400	2.052	VW	400
1.95	M	222	1.954	VW	222
1.91	M	312	1.901	M	312
1.83	MS	213	1.848	M	213
			1.882	W	230
1.81	W	410	1.790	M	410
1.77	MS	402	1.765	M	402

and EPMA was difficult because there was a considerable variation in composition across the crystal. A crystal of $Er_2Si_2O_7$ was used as a standard for EPMA. The formulae of the limiting compositions, derived from EPMA, have been expressed in the apatite form (Table II). The Er-rich form is $Pb_{1.4}Er_{2.93}Si_{3.6}O_{13}$ and the Pb-rich form, $Pb_{1.8}Er_{2.5}Si_{3.7}O_{13}$. If the structure indeed corresponds to that of apatite, the Si in excess of 3 in the formula then occupies the large cation sites together with Pb and Er. The extent of compositional variation of compound B is indicated in Fig. 2.

One or both phases crystallized between the regions A and B, sometimes with Er_2SiO_5.

4.4. Experiments with R = Y, Dy, Gd

Starting compositions, similar to those which produced $PbEr_4Si_5O_{17}$ but with Er_2O_3 replaced by Dy_2O_3 and Y_2O_3, gave crystals with closely related powder patterns. A starting composition is given in Table I(d) and X-ray powder pattern data in Table V. With Gd, phase A was not obtained; when R had an ionic radius larger than Er and Y, the apatite-related phase crystallized from compositions higher in SiO_2.

Preliminary susceptibility measurements indicate that $PbDy_4Si_5O_{17}$ undergoes a transition to an antiferromagnetic state at 1.2 K [16].

Acknowledgements

The authors are grateful to Dr G. Garton for helpful discussions and to Dr S. H. Smith for technical assistance. This work was supported in part by the Science Research Council.

References

1. I. A. BONDAR and N. A. TOROPOV, *Mat. Res. Bull.* **2** (1967) 479.
2. G. J. MCCARTHY, W. B. WHITE and R. ROY, *J. Inorg. Nucl. Chem.* **29** (1967) 253.
3. YU.I. SMOLIN and YU.F. SHEPELEV, *Acta Cryst.* **B26** (1970) 484.
4. L. A. HARRIS and C. B. FINCH, *Amer. Minerol* **50** (1965) 1493.
5. J. FELSCHE and W. HIRSIGER, *J. Less-Common Metals* **18** (1969) 131.
6. J. FELSCHE, *ibid* **21** (1970) 14.
7. YU.I. SMOLIN and S. P. TKACHEV, *Sov. Phys. Crystallog.* **14** (1969) 175.
8. C. MICHEL, G. BUISSON and E. F. BERTAUT, *Compt. Rend. Acad. Sci. Paris* **264B** (1967) 397.
9. B. M. WANKLYN, F. R. WONDRE, G. B. ANSELL and W. DAVISON, *J. Mater. Sci.* **9** (1974) 2007.
10. J. FELSCHE, "The Crystal Chemistry of the Rare Earth Silicates", in "Structure and Bonding", Vol. 13 (Springer-Verlag, New York, 1973) pp. 99-197.
11. E. M. LEVIN, R. ROBBINS and H. F. MCMURDIE, "Phase Diagrams for Ceramists", 1969 Supplement (American Ceramic Society, Columbus, Ohio, 1969).
12. G. GARTON, S. H. SMITH and B. M. WANKLYN, *J. Crystal Growth* **13/14** (1972) 588.
13. B. M. WANKLYN and Z. HAUPTMAN, *J. Mater. Sci.* **9** (1974) 1078.
14. B. M. WANKLYN and G. GARTON, *ibid* **9** (1974) 1378.
15. S. SWITHENBY, B. M. WANKLYN and M. R. WELLS, *ibid* **9** (1974) 845.
16. A. H. COOKE and J. SILVA, Clarendon Laboratory, private communication.

Received 31 January and accepted 17 February 1975.